Accepted Manuscript

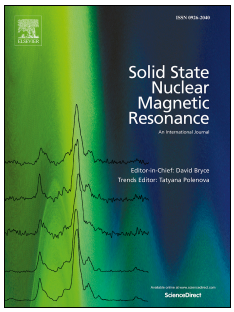

Acetone mobility in zeolite cages with new features in the deuteron NMR spectra and relaxation

E.E. Ylinen, M. Punkkinen, A. Birczyński, Z.T. Lalowicz

PII: S0926-2040(18)30025-0

DOI: 10.1016/j.ssnmr.2018.05.001

Reference: YSNMR 838

To appear in: *Solid State Nuclear Magnetic Resonance*

Received Date: 13 March 2018

Revised Date: 16 May 2018

Accepted Date: 16 May 2018

Please cite this article as: E.E. Ylinen, M. Punkkinen, A. Birczyński, Z.T. Lalowicz, Acetone mobility in zeolite cages with new features in the deuteron NMR spectra and relaxation, *Solid State Nuclear Magnetic Resonance* (2018), doi: 10.1016/j.ssnmr.2018.05.001.

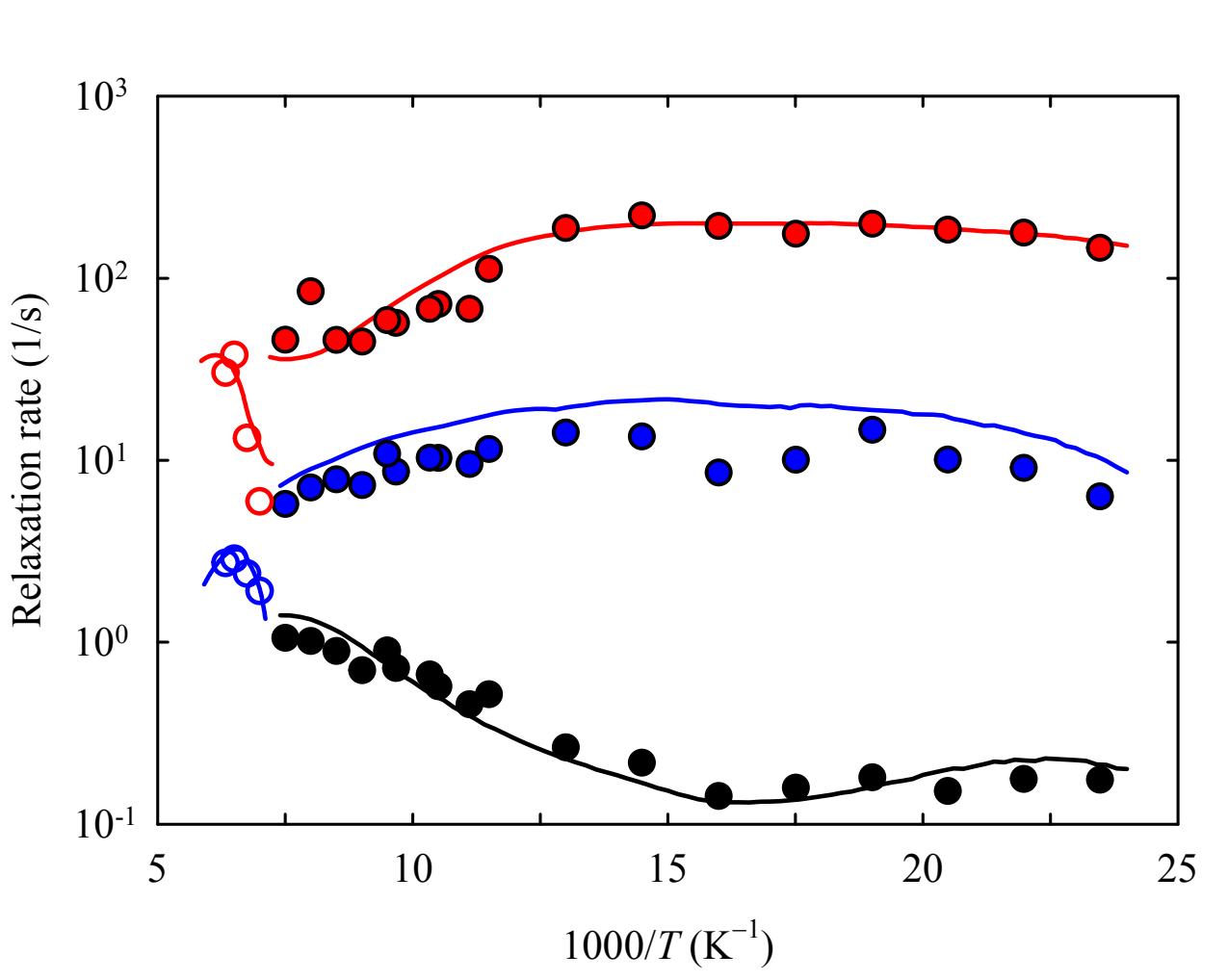
Relaxation rate (1/s)
10^3
10^2
10^1
10^0
10^-1
5
10
15
20
25
1000/T (K^-1)

Acetone mobility in zeolite cages with new features in the deuteron NMR spectra and relaxation

E.E. Ylinen [a,*], M. Punkkinen [a], A. Birczyński [b], Z.T. Lalowicz [b]

[a] Wihuri Physical Laboratory, Department of Physics and Astronomy, University of Turku, FI-20014 Turku, Finland

[b] H. Niewodniczański Institute of Nuclear Physics of PAS, ul. Radzikowskiego 152, 31-342 Kraków, Poland

*Corresponding author
Dr. Eero Ylinen
Wihuri Physical Laboratory, Department of Physics and Astronomy
University of Turku, FI-20014 Turku, Finland
E-mail address: eero.ylinen@utu.fi

Abstract

We studied deuteron NMR spectra and spin−lattice relaxation of deuterated acetone-d_6, adsorbed into zeolites NaX(1.3) and NaY(2.4) at 100 % coverage of sodium cations. At temperatures roughly below 160 K the deuterons are localized and their NMR characteristics are determined by CD_3 rotation and rotational oscillations of acetone molecules. In NaX the CD_3 rotation and rotational oscillations about the twofold axis of acetone dominate the spectra below 100 K, while above it oscillations also about other axes become important. In NaY dominant features are related to methyl tunnelling and to a smaller extent to rigid acetones, before the rotational oscillations about twofold axis start to prevail above 40 K. The analysis of the strongly non-exponential magnetization recovery was done by applying the recently introduced method (Ylinen et al., 2015 [12]), improved here to take into account the limited fast recovery at the level crossings, 10 % at $\omega_t = \omega_0$ and 28 % at $\omega_t = 2\omega_0$. At first the experimental recovery is fitted by three exponentials with adjustable weights and decay rates. Then these quantities are calculated from activation energy distributions and known expressions for the deuteron relaxation rate. In NaY two distinctly separate activation energy distributions were needed, the dominant one being very broad. The use of three distributions, two of them covering practically the same energies as the broad one, lead to a somewhat better agreement with experiment. In general the theoretical results agree with experiment within experimental scatter. As the final result the mean activation energies and widths are obtained for activation energy distributions.

Key words: non-exponential NMR relaxation; activation energy distribution; decreasing activation energy; rotational tunnelling; acetone in zeolite; deuteron NMR spectra; molecular mobility; methyl group

1. Introduction

Numerous studies have been carried out on the structure and motional properties of solids by observing the deuteron NMR spectra and spin–lattice relaxation. Especially such samples were investigated, which contain deuteron tetrahedra or CD_3 groups. Rotational tunnelling changes their spectra and relaxation in a characteristic way at low temperatures [1−8]. Translational symmetry results in identical surrounding and potential for all rotators in solids and the molecular mobility is uniform for all. Relaxation rate maxima reflect rotational mobility in well-defined potentials.

There is no translational symmetry in zeolites because molecules interact with different adsorption centers and are located at different positions. Therefore zeolites show many interesting properties and their role as industrial catalysts has inspired an enormous number of studies. Usage of guest molecules and investigation of their adsorption at molecular level is one of the ways to characterize zeolites. Guest–host interactions have important implications and stimulate investigation in this field [9].

We apply deuteron NMR methods to investigate molecular motions in confinement in a wide range of temperature. Effects related to translational mobility were observed at high temperature, followed by the onset of molecular reorientations. Molecules become localized at a temperature, defined in the following as T_S, which appears to be an important parameter related to the strength of molecular interactions with zeolite framework. The rotations of guest molecules and their subgroups alone determine the deuteron spectral shape and their spin−lattice relaxation below T_S. Thus by studying a single sample with molecules in confinement we may observe features characteristic for gaseous, liquid and finally like in solid state. Results for representative set of molecules were summarized in a recent publication [10].

Somewhat random replacement of Si atoms by Al atoms in zeolites makes the surroundings of guest molecules vary in a statistical way, which causes a distribution for example in the potential hindering the methyl rotation of such molecules. Recent results on methyl-containing zeolites NaX and NaY reveal that this distribution can be observed in the deuteron spin−lattice relaxation of localized methyl groups below T_S as a pronounced non-exponentiality [11, 12]. Such non-exponentiality is not only a property of guest molecules in zeolites but it can be observed in many other materials like polymers, glasses and other disordered materials. The effect of the underlying distribution of the relevant motional process on the NMR spectra was explained theoretically rather early [13, 14]. There are also several studies, which derive characteristic motional parameters like the mean activation energy and the distribution width from the magnetization recovery [15−18]. However, they concentrate mainly on processes, where rotational tunnelling does not play any role and one distribution is sufficient to describe the experimental data. Many CD_3 containing molecules in zeolites, studied so far, are located at clearly non-equivalent positions. In such a case the description of the activation energies requires two or more distributions centered about at least two clearly different mean activation energies. In the acetone molecule the methyl groups are equivalent but their varying surroundings in NaX and NaY mean that quite probably we need two activation energy distributions, with distinctly different mean activation energies.

Our method for analysing non-exponential deuteron relaxation of methanols in confinement was published some time ago [11, 12]. It takes into account the effect of rotational tunnelling and can be applied in the presence of many activation energy distributions. It requires a rather accurate simulation of the experimental magnetization

recovery. Often the experimental data are described very well by the so-called stretched exponential function $\exp[-(t/T_c)^b]$ when the parameters T_c and b are properly adjusted. Usually b is near 0.5, in any case clearly smaller than 1. Unfortunately, there is so far no theoretical method for calculating T_c and b, which prevents the comparison between theory and experiment. Therefore, we use a number of exponential function $\exp(-Rt)$, which do not have this drawback. At low temperatures three exponentials are used to describe the magnetization recovery, with the rates R and weights as adjustable parameters. These can also be calculated theoretically as described in [11, 12] and in sections 2 and 5. Experimental scatter prevents the sufficiently accurate extraction of rates and weights when four or more exponentials are used, although that would improve the accuracy of our method in principle. Within a certain temperature range near T_S the relaxation data could be described quite accurately with two exponentials.

In the present study we use basically the same method as in [11, 12] but introduce one improvement. At low temperatures it may happen that the deuteron resonance frequency ν_0 is equal to the tunnel frequency $\nu_t = \omega_t/2\pi$ or to $\nu_t/2$. Then the relaxation proceeds partially very fast. Earlier estimates for the degree of the fast relaxation have been too large. In the present study we derive estimates for this degree, which are believed to be valid in the absence of any appreciable spin diffusion between deuterons.

Our special interest is deuteron NMR spectra and spin−lattice relaxation of totally deuterated acetone-d_6 in NaX and NaY. Some earlier studies deal with the ^{13}C chemical shift of acetone complexes at Brønsted and Lewis acid sites [19−21]. It was pointed out that both temperature and surface coverage are critical for the acetone mobility and interaction at these sites [22]. One may expect rotational freedom for methyl groups and certain mobility about the twofold axis of such localized acetone molecules. Particularly interesting seems to be the rather complicated mobility of acetone dimers [19].

2. Deuteron spin−lattice relaxation

To study the spin−lattice relaxation of methyl deuterons in the case, when there is a broad activation energy distribution, we use basically the same method as in two recent investigations [11, 12]. The only significant modification concerns the degree of the magnetization recovery via so-called level-crossing transitions.

As mentioned before, the two CD_3 groups of an acetone molecule in zeolite can be non-equivalent. Therefore the methyl groups experience the hindering potential $V(\phi) = (V_3/2)(1 - \cos 3\phi)$ with different barrier heights V_3. We do not consider possible sixfold or higher symmetry terms in the potential. For each V_3 the Mathieu equation is solved and the rotational energies E_r for the ground (r = 0) and excited torsional states (r = 1, 2, etc) are obtained. The corresponding conventional activation energy is $A_0 = V_3 - E_0$. Though the starting point for this approach is the potential strength V_3, the just defined activation energy A_0 was taken as the variable quantity. The additionally needed quantities, the "activation energies" $A_r = E_r - E_0$ and the tunnel frequencies $\omega_{rt} = (E_{rEa} - E_{rA})\ /\ \hbar$ for the various rotational levels r, were calculated as a function of A_0 [12]. Also the temperature dependence of the ground-state tunnel frequency $\omega_t = (E_{0Ea} - E_{0A})\ /\ \hbar$ was obtained. Then the corresponding correlation time for the 120° jumps about the methyl axis was calculated from

$$\frac{1}{\tau} = K_h|\omega_{bt}| \exp\left(-\frac{A_0}{RT}\right) + K_l \sum_r |\omega_{rt}| \exp\left(-\frac{A_r}{RT}\right) \qquad (1)$$

Here ω_{bt} is the tunnel frequency for such an excited-state energy $(E_{\mathrm{rEa}} + E_{\mathrm{rA}})/2$, which equals the barrier height V_3. The first term of this expression is the conventional Arrhenius equation, with $\mathrm{K_h}|\omega_{\mathrm{bt}}|$ corresponding to the pre-exponential factor. The second term describes the well-known fact that at low temperatures the variation of the correlation time τ requires a constantly decreasing activation energy [23−27]. The two parameters $\mathrm{K_h}$ and $\mathrm{K_l}$ are numerical factors within one order of magnitude from 1.

Especially for low activation energies A_0 and low temperatures, where the tunnel frequency ω_{t} can equal the deuteron resonance frequency ω_0, the well-known expression for the orientationally averaged spin−lattice relaxation rate of the methyl deuterons

$$R(\tau) = \frac{\omega_{\mathrm{Q}}^2}{15}[\mathrm{J}(\tau,\omega_0) + 4\mathrm{J}(\tau,2\omega_0)] \tag{2}$$

with $\mathrm{J}(\tau,\omega) = \tau/(1+\omega^2\tau^2)$, is no more applicable. In Supplemental Material of [12] the relaxation of the A and E species magnetizations, M_{A} and M_{E} respectively, was considered. According to the earlier study they are coupled significantly only to the rotational polarization and the tunnelling reservoir (= the difference between the populations of the A and E species levels) [8]. The former coupling can be important only in the fast-motion region $\omega_0\tau < 1$, but since all the discussed quantities relax there roughly at the same rate, this coupling could be ignored. The coupling to the tunnelling reservoir is expected to be important only when ω_{t} and ω_0 are of same magnitude. Then the orientationally averaged relaxation rates

$$R_{\mathrm{Ain}} = \frac{\omega_{\mathrm{Q}}^2}{30}[\mathrm{J}(\tau,\omega_{\mathrm{t}}+\omega_0) + \mathrm{J}(\tau,\omega_{\mathrm{t}}-\omega_0) + 4\mathrm{J}(\tau,\omega_{\mathrm{t}}+2\omega_0) + 4\mathrm{J}(\tau,\omega_{\mathrm{t}}-2\omega_0)]$$

$$R_{\mathrm{Ein}} = \frac{\omega_{\mathrm{Q}}^2}{120}[6\mathrm{J}(\tau,\omega_0) + \mathrm{J}(\tau,\omega_{\mathrm{t}}+\omega_0) + \mathrm{J}(\tau,\omega_{\mathrm{t}}-\omega_0) + 24\mathrm{J}(\tau,2\omega_0) + 4\mathrm{J}(\tau,\omega_{\mathrm{t}}+2\omega_0) + 4\mathrm{J}(\tau,\omega_{\mathrm{t}}-2\omega_0)] \tag{3}$$

could be used for the magnetizations M_{A} and M_{E} under the condition that the damping rates for the so-called Kramers and tunnelling coherences, $\mathrm{k_K}$ and $\mathrm{k_t}$ respectively, are equal to each other and also equal to the inverse correlation time $1/\tau$ [28].

It is important to realize that in the fast-motion region both expressions in (3) reduce to (2). If at low temperatures $\omega_{\mathrm{t}} \gg \omega_0$ and $\omega_0\tau \gg 1$, R_{Ein} and R_{Ain} are still applicable [12]. Only when ω_{t} and ω_0 are roughly equal, the relaxation process becomes more complicated. Still a certain part of the total magnetization $M_z = M_{\mathrm{A}} + M_{\mathrm{E}}$ relaxes very fast via the level-crossing transitions. They change the energy by $\omega_{\mathrm{t}} - \omega_0$ and $\omega_{\mathrm{t}} - 2\omega_0$, which may be very small in comparison with ω_0. Therefore the corresponding transition rates are clearly larger than the other rates. The remaining part of M_z relaxes roughly at the rate determined by the transitions not involving level crossings [12 and its Supplemental Material], the process being most probably highly multiexponential. In the previous study [12] the expressions (3) were used also in this case, but with the modification that in the spectral density functions $\mathrm{J}(\tau,\omega_{\mathrm{t}}-\omega_0)$ and $\mathrm{J}(\tau,\omega_{\mathrm{t}}-2\omega_0)$ of

R_{Ain} the differences $\omega_{\mathrm{t}} - \omega_0$ and $\omega_{\mathrm{t}} - 2\omega_0$ were replaced by $\omega_0/2$ as soon as their absolute values became smaller than $\omega_0/2$. In this way the effect of the fast level-crossing transitions was removed from the final stage of the relaxation. In R_{Ein} the quite different replacement was done by replacing the mentioned frequency differences by $\omega_{\mathrm{d}} = 2\pi{\cdot}160{\cdot}10^3$ 1/s, when their absolute value became smaller than ω_{d}. This is a consequence of the quadrupole coupling, which causes the smallest separation between the apparently crossing A and E species levels to be of that magnitude.

The quadrupole interaction does not become completely time-dependent via rotation about the threefold methyl axis. Actually the fast methyl rotation averages the quadrupole interaction to one third of its motionless value as demonstrated for example by the spectral data in section 4. When the acetone molecule starts to move at higher temperatures, also the remaining part becomes at least partly time-dependent. This causes an additional contribution R_{mol} to the relaxation of the methyl deuterons, approximately similar to Eq. (2) above, but with τ representing the molecular correlation time and the multiplier 1/15 replaced by a smaller one. The maximum value of this factor is 1/120 when the acetone motion makes the entire quadrupole coupling time dependent. In reality the motion is not sufficiently isotropic and therefore the multiplying factor is left as a parameter.

In practice the analysis of the deuteron relaxation experiments and the numerical calculation proceeds in the following way. The magnetization recovery after the saturation is described by a sum of three exponentials with adjustable weights w_{f}, w_{m} and w_{s} and characteristic relaxation rates R_{f}, R_{m} and R_{s} for the fast, intermediate and slow component, respectively. From the characteristic rates we calculate limiting values $L_{\mathrm{fm}} = \sqrt{R_{\mathrm{f}}R_{\mathrm{m}}}$ and $L_{\mathrm{ms}} = \sqrt{R_{\mathrm{m}}R_{\mathrm{s}}}$ as a function of temperature. We introduce four parameters for a methyl group, the mean activation energy A_0, the distribution width σ and the numerical factors K_{h} and K_{l}. The methyl activation energy is defined by $A_{\mathrm{j}} = A_0 + \mathrm{j}\Delta A$, where j = ... −3, −2, −1, 0, 1, 2, 3... and ΔA is the incremental change. Then all the needed quantities for calculating the methyl correlation time τ and the relaxation rates R_{Ain} and R_{Ein} are estimated as described above and in [12], with the mentioned modifications. A distributed activation energy is also included to describe the motion of the acetone molecule. Three additional parameters (A_0', σ′ and the pre-exponential factor) are needed and the corresponding activation energy is defined by $A_{\mathrm{k}}' = A_0' + \mathrm{k}\Delta A'$, where k = ... −3, −2, −1, 0, 1, 2, 3... and $\Delta A'$ is the incremental change. The corresponding rate R_{mol} is then calculated. It is worth noticing that R_{mol} at maximum contains only the part 1/9 of the total relaxing power of the methyl deuterons. Therefore it is rarely taken into account, it was not considered in our earlier studies, either [11, 12]. The individual total relaxation rate is $R_{\mathrm{Ain}} + R_{\mathrm{mol}}$ (or $R_{\mathrm{Ein}} + R_{\mathrm{mol}}$).

The corresponding weight is denoted $w_{\mathrm{Ajk}} = (5/9)w_{\mathrm{j}}w_{\mathrm{k}}$. The subscripts j and k refer to methyl and acetone motions, respectively. For an E species methyl group the corresponding weight is $w_{\mathrm{Ejk}} = (4/9)w_{\mathrm{j}}w_{\mathrm{k}}$. The multipliers 5/9 and 4/9 are related to the fact that at thermal equilibrium the relative weights of the magnetizations M_{A} and M_{E} are 5/9 and 4/9, respectively. The weights w_{Ajk} and w_{Ejk} have still to be multiplied by the numerical factor w_{n}, which means the probability of occupation of the certain position by an acetone molecule in zeolite. This factor equals ½, if there are equally many methyl groups in two non-equivalent methyl positions. w_{j} is determined by the Gaussian distribution for the methyl activation energy A_{j} as

$$w_{\mathrm{j}} = \exp[-(\mathrm{j}\Delta A)^2/2\sigma^2]/\textstyle\sum_{\mathrm{j}}\exp[-(\mathrm{j}\Delta A)^2/2\sigma^2] \qquad (4)$$

A similar expression is used for the weight w_k, which is related to the activation energy distribution of the acetone molecule. Finally the obtained value for example for the characteristic rate of the intermediate component is

$$R_m = \sum_{njk} w_n \left[w'_{Ajk} \left(R_{Ain,j} + R_{mol,k} \right) + w'_{Ejk} \left(R_{Ein,j} + R_{mol,k} \right) \right] / w_m \qquad (5)$$

where the corresponding relative weight is $w_m = \sum_{njk} w_n \left(w'_{Ajk} + w'_{Ejk} \right)$. The prime as a superindex in weights means that only such total relaxation rates are taken into account, which fall between L_{fm} and L_{ms}. The weights and characteristic rates are calculated as a function of temperature and compared with the experimental ones, then the 11 parameters are changed somewhat to reach a better agreement with the experimental data until the best possible agreement is reached. The resulting 11 parameters describe the rotational motion of the acetone molecule and its two methyl groups in the zeolite.

Actually the mentioned relative weights are problematic in the level-crossing region. It is all right to use the relative weight $w_{Ejk} = (4/9) w_j w_k$ for the E species methyl groups when ω_t is much smaller or larger than ω_0. However, features related to level-crossing transitions, when ω_t is of the same magnitude as ω_0, are very difficult to observe even in single crystals, where the activation energy distribution is very narrow. In the presence of a broad distribution almost no signs of level crossing can be observed in the relaxation, the maximum effect being a small increase in the overall relaxation rate within a certain temperature range. Therefore, the multiplier 4/9 is too large in this region. The practically vanishing spin diffusion between deuterons of neighbouring CD_3 groups at low temperatures invalidates the normal theoretical derivations, which are based on various spin temperatures [4−8]. In Supplemental Material we present, by using the results of [29], a different but simple approach to calculate the upper limit, to which the relaxation process of the magnetization can proceed via the relevant level-crossing transitions. It turns out that at $\omega_t = \omega_0$ and near it the fast relaxation recovers 10.2 % of the total magnetization M_{eq}, while at $\omega_t = 2\omega_0$ the corresponding limit is 28.1 %. These modify Eq. (5) causing the following changes in R_{Ein} and the corresponding weight w_{Ejk} in the region, where the tunnel frequency ω_t lies between $\omega_0/2$ and $5\omega_0/2$. Otherwise the calculations proceed as described above, also R_{Ain} and w_{Ajk} remain unchanged. Thus,
(a) when $\omega_0/2 < \omega_t < 3\omega_0/2$, one part of deuterons relaxes at the rate $R_{Ein} + R_{mol}$, with the relative weight $0.102 w_j w_k$ replacing w_{Ejk} in (5) and $R_{Ein,j}$ equal to the unchanged expression in Eq. (3). Still $\omega_t - \omega_0$ is replaced by ω_d in the denominator of the spectral density function $J(\tau, \omega_t - \omega_0)$ if the absolute value of $\omega_t - \omega_0$ is smaller than ω_d. For another part the relative weight $(4/9 - 0.102) w_j w_k$ replaces w_{Ejk} in (5) and $R_{Ein,j}$ is modified so that the difference $\omega_t - \omega_0$ in the spectral density function is replaced by $\omega_0/2$.
(b) When $3\omega_0/2 < \omega_t < 5\omega_0/2$, one part of deuterons relaxes at the rate $R_{Ein} + R_{mol}$, with the relative weight $0.281 w_j w_k$ replacing w_{Ejk} in (5) and $R_{Ein,j}$ equal to the unchanged expression in Eq. (3). Still $\omega_t - 2\omega_0$ is replaced by ω_d in the spectral density function $J(\tau, \omega_t - 2\omega_0)$ if the absolute value of $\omega_t - 2\omega_0$ is smaller than ω_d. For another part the relative weight $(4/9 - 0.281) w_j w_k$ replaces w_{Ejk} in (5) and $R_{Ein,j}$ is modified so that the difference $\omega_t - 2\omega_0$ in $J(\tau, \omega_t - 2\omega_0)$ is replaced by $\omega_0/2$.
In calculations we used the value $\omega_d/2\pi$ = 160 kHz.

3. Experimental details

Zeolites NaX(1.3) (supplied by Sigma-Aldrich) and NaY (2.4) (purchased from Linde company) were activated *in situ* in an NMR sample tube. The sample was first evacuated at room temperature for 30 min, and then the temperature was raised, at the rate of 5 K/min, to 700 K and kept there in vacuum for 1 h. The doses of $(CD_3)_2CO$ were adsorbed into the zeolite up to 100% of the total coverage of Na^+ ions. The doses were determined by controlling the acetone pressure to the accuracy of 100 Pa. All the samples were sealed in 24 mm long glass tubes with the outside diameter 5 mm.

The NMR experiments were carried out over a range of temperatures regulated by the Oxford Instruments CT503 Temperature Controller to the accuracy of ±0.1 K. The static magnetic field 7 T was created by the superconducting magnet made by Magnex, and the ^{2}H resonance frequency was equal to 46 MHz. The NMR probe was mounted inside the Oxford Instruments CF1200 Continuous Flow Cryostat. Pulse formation and data acquisition were provided by Tecmag Apollo 500 NMR console. The dwell time was set to 1 μs. The π/2 pulse equal to 3 μs assured the uniform excitation [30] for our 200 kHz spectra.

NMR spectra were obtained by the Fourier Transformation of the Quadrupole Echo (QE) signal. The sequences $(\pi/2)_x - t_d - (\pi/2)_y - t_{rep}$ were used, the pulse separation time t_d being of the order of 50 μs. The time t_d was adjusted by means of the home-designed code for Tecmag console in order to optimize QE signal intensity for each temperature. The phase cycling sequence was applied and focused on the FID signal cancellation in the overall signal after the quadrupole echo sequence. For the relaxation time measurements we used the saturation−recovery quadrupole-echo pulse sequence $[(\pi/2)_x - \tau_n]^n - t_{var} - (\pi/2)_x - t_d - (\pi/2)_y - t_{rep}$. The relaxation measurements yielded a set of signal amplitudes which directly led to the magnetization recovery curve $M_z(t_{var})$. The QE amplitudes at the maximum were recorded. In the case of non-exponential relaxation the magnetization recovery was fitted into a combination of three exponentials $M_z(t) = \sum_{i=1-3} M_i[1 - \exp(-R_i t)] + c_0$ by using the least-squares method. The sum $M_1+M_2+M_3+c_0$ is equal to the equilibrium magnetization M_∞. The parameter c_0 takes into account that the saturation may not always be perfect. The relative weights w_i are calculated from M_i, for example the relative weight w_1 of the exponential $\exp(-R_1 t)$ equals $w_1 = M_1/(M_1 + M_2 + M_3)$. In the case of biexponential recovery the third term containing M_3 was ignored.

Two temperature ranges with significantly different molecular dynamics, above and below a temperature defined as T_S, are the common feature for molecules in confinement. Translational and rotational mobility drives the relaxation process above T_S and narrow spectra are observed. Molecules become localized below T_S. If T_S is determined from the broadening of the deuteron spectrum, we obtain the results 164 K and 159 K for NaX and NaY, respectively. However, multiexponential deuteron relaxation may sometimes make that determination somewhat uncertain. Alternatively we may define T_S as the lowest temperature, where the relaxation measurements are possible by FID, thus QE methods are applied below T_S.

4. Deuteron spectra

Taking into account a molecule with CD_3 groups one may expect a set of characteristic spectra. For immobile methyl deuterons with long rotational correlation times ($\tau_c \gg 10^{-6}$ s) the Pake doublet is observed. The doublet separation equals $\frac{3}{4}C_Q$ ($C_Q = e^2qQ/h$), what provides the value of quadrupole coupling constant. Rotation of the methyl group leads to the doublet with the separation equal to $\frac{1}{4}C_Q$. The appearance of a sideband is a fingerprint of tunnelling rotation [2]. The asymmetry parameter η was taken equal to zero in all these spectra. The spectra of acetone $(CD_3)_2CO$, as it will be shown below, consist of spectral components with $\eta \neq 0$ (Fig.1). That we consider as an evidence for spectral averaging by torsional jumps. Respective spectra with a jump amplitude as a parameter were calculated using WEBLAB package available on internet [31].

Let us consider an acetone molecule in the Cartesian reference frame, with the Z axis parallel to the two-fold symmetry axis of acetone (thus joining the C−O bond). The Y axis lies in the plane containing the three carbons, while the X axis is perpendicular to that plane. Guided by experimental spectra we consider torsional oscillations about the two-fold axis first. With the oscillation amplitude 42º we obtain the spectrum labelled as (Z) in Fig. 1. Additional rotational oscillations with the amplitude 66.7º of the molecular plane about the Y axis provide the spectrum (Z,Y) in Fig. 1. If the additional oscillations take place about the X axis (instead of Y), the obtained spectra do not resemble the experimental ones. Torsional oscillations about the X axis with the amplitude 79.5º, in addition to those about the Z and Y axes, provide the spectrum labelled (Z,Y,X) in Fig. 1. All the spectra in Fig. 1 have the asymmetry parameter significantly different from zero, $\eta = 0.161$ for the spectrum (Z), $\eta = 0.606$ for (Z,Y) and $\eta = 0.322$ for (Z,Y,X). These spectra will be used in fitting the experimental spectra. They appear with increasing temperature and we will use in the following the new labels lt, mt and ht for (Z), (Z,Y) and (Z,Y,X), respectively. It is worth noticing that the deuteron spectra with $\eta > 0$ were observed for acetone-d_6 in some inclusion compounds. The spectra obtained at the lowest temperature yielded the value $\eta = 0.14$, which is close to our value for the lt spectrum. However, the interpretation of the asymmetry parameter was based on a deformation of the methyl group structure, which is not convincing [32, 33].

4.1. Acetone spectra in NaX

We take T_S = 164 K as QE methods were applied in relaxation measurements from 165 K downwards. However, in addition to narrow Gaussian, some other spectral components were observed at 180 K (Fig. 2). Namely the components ht and mt are clearly recognizable. The component lt appears at 120 K and dominates the spectra on decreasing temperature. Two Pake doublets, with C_Q equal 170 kHz and 105 kHz, respectively, are visible in the spectra at the lowest temperature. The temperature dependence of the contributions of the spectral components is shown in Fig. 3. The Pake doublets exist up to about 66 K, while the contribution of lt remains constant at 70% in this range. The component mt increases systematically from about 20 K up to about 45%, as does also the ht component roughly above 35 K.

On the other hand the mt and ht components are present from low temperatures. Methyl groups are rotating in molecules subjected to torsional oscillations. The components mt and ht seem to emerge at the expense of Pake doublets. The onset of methyl rotation uncovered torsional degrees of freedom. Inspection of the related contributions discloses intensity transfer from the Pake doublet with C_Q = 170 kHz into mt components (Fig. 3). The reduced quadrupole coupling constant for the second Pake

doublet may reflect an effect of torsional oscillations. That component converts into ht on increasing temperature.

4.2. Acetone spectra in NaY

Representative spectra, measured below 159 K, are shown in Fig. 4. The spectral component of tunnelling methyl groups dominates with 60% contribution at lowest temperature. Two Pake doublets are also seen, with the coupling parameters C_Q = 177 kHz (30% contribution) and C_Q = 107 kHz (7%). The methyl tunnelling component is visible up to about 50 K. The contribution of the broader Pake doublet decreases significantly above 40 K. The component lt appears at about 25 K. Its contribution increases first at the expense of the tunnelling component, then further increase comes from the broad Pake doublet and finally it exceeds 90% at highest temperature. Other spectral components play a marginal role (Fig. 5).

There is no visual evidence for torsional oscillations in the shape of the spectra of tunnelling methyl groups. Potential hindering their rotation is very low. On the other hand, there are also sites where this potential is sufficiently high to make deuterons practically immobile. All methyl groups rotate above 50 K in molecules undergoing torsional oscillations about the twofold symmetry axis.

4.3. Comparative discussion of spectra

Some of the spectral features in NaX and NaY and their differences are naturally related to acetone bonding and surroundings in zeolites. It should be understood that the observed spectral changes as a function of temperature take place over a relatively large temperature range because of the broad activation energy distributions.

The sample of NaX (Si/Al = 1.8) contains 85 acetone molecules per unit cell, located probably mostly in supercages, and their number equals that of sodium cations. In the case of NaY (Si/Al = 2.4) we have 56 sodium cations compensating the charge of equal number of aluminium atoms in the zeolite framework. Acetone molecules can be bonded to sodium cations via the free electron pair of oxygen. Such interaction is much stronger in NaY than in NaX [34]. We have to consider also the hydrogen bonding of acetone deuterons with the framework oxygen atoms. These atoms are less negative in NaY than in NaX due to a smaller number of AlO_4 tetrahedra, thus hydrogen bonds are relatively weaker for NaY. The lower value of T_S for NaY indicates the dominating role of the hydrogen bonding in the process of acetone immobilization. Similarly the value of T_S for CD_3OD molecules was found to be lower in NaY than in NaX [35], however the difference in T_S was significantly bigger. That may refer to a more significant, competing role of bonding to sodium cations in the case of acetone.

The mobility of methyl deuterons differs significantly in NaX and NaY at lowest temperatures. We have the dominating lt component (70 % at 20 K) accompanied by remaining rigid deuterons in NaX. The component lt may be attributed to the acetone molecules bonded to sodium cations at vertical positions with respect to cage walls. There is a potential with twofold symmetry for torsional oscillations. Acetone molecules at other positions have methyl groups immobilized via hydrogen bonds to framework oxygens. There is a higher abundance of acetone molecules in NaX than NaY, mutual interactions may be expected, and the twofold potential for molecules in the vertical positions may come from neighbouring molecules. The contributions mt and ht are visible for NaX from relatively low temperature, and they increase systematically on

expense of Pake doublets and lt component above 70 K. Finally mt and ht dominate the spectra at highest temperatures, accompanied by a Gaussian component from isotropically reorienting molecules.

Lower abundance of sodium cations in NaY may lead to new local conditions as the interaction with sodium cations is stronger and acetone molecules are located closer to them. Most of acetones are found at horizontal positions with one methyl group immobilized and the second one relatively free, thus exhibiting tunnelling rotation. The spectrum of the tunnelling methyl groups dominates (60 % at 10 K), the remaining contributions representing Pake doublets. The contribution of that component should amount to 50 %, which is close to the experimental value within expectable error. The Pake doublet (177 kHz), with the contribution of about 33 % at low temperature, starts to decrease at about 33 K, but is still visible somewhat above 100 K. Due to a relatively stronger bonding to sodium cations in this case, acetone molecules are kept at horizontal position more strongly. The component lt starts to dominate the spectrum above 40 K on the expense of Pake doublets, with a related decrease of the tunnelling methyl component. Thus on increasing temperature acetone molecules seem to change their orientation with respect to the cage walls from the horizontal to vertical position.

5. Spin−lattice relaxation of acetone deuterons in NaX and NaY

5.1. Experimental results for NaX and NaY

The fitting of the magnetization recovery curves with three exponential functions leads to numerical values for the three relaxation rates R_i and the three relative weights w_i. The results are shown in Figs. 6 and 7 for NaX and in Figs. 8 and 9 for NaY. Above 85 K in NaX and 140 K in NaY two exponentials were sufficient to describe the growing magnetization quite accurately (Figs. 6 and 8).

In NaX the relaxation rate of each exponential (also called component) increases at first when temperature is lowered, reaches a flat maximum between 60 K and 33 K and then starts to decrease. The maximum of the smallest rate R_s is narrower than those of the fast and intermediate components, R_f and R_m, respectively, and occurs near 60 K. The weight w_f of the fast component shows a maximum near 38 K, while w_m is practically constant at higher temperatures and then decreases steadily with temperature. The weight w_s shows a minimum near 40 K but then grows steadily to 0.5 near 21 K. In the two-exponential region both the rates decrease when temperature is raised. The weight of the faster component shows a maximum near 115 K.

In NaY the relaxation rate of the fast component R_f increases at first when temperature is lowered and becomes then practically constant below 77 K (Fig. 8). R_m is almost independent of temperature, while R_s decreases at first with temperature and becomes then nearly constant. The weight w_f has a maximum near 63 K (Fig. 9), resembling the variation of w_f in NaX. w_m decreases at first with temperature but varies only slightly at lower temperatures. w_s decreases at first slightly with temperature, shows a broad minimum and then starts to grow below 63 K. In the two-component region above 140 K the relaxation rate of the fast component increases with temperature, while the variation of the slow component is clearly smaller. The weight of the slow component increases with temperature and is nearly 90 % above 150 K.

5.2. Calculations and discussion for NaX

The numerical calculations require the limiting values $L_{\mathrm{fm}} = \sqrt{R_{\mathrm{f}}R_{\mathrm{m}}}$ and $L_{\mathrm{ms}} = \sqrt{R_{\mathrm{m}}R_{s}}$, which were calculated for each experimental temperature. Their logarithms were fitted with polynomial functions. In simulations we used the quadrupole coupling frequency $\nu_{\mathrm{Q}} = \omega_{\mathrm{Q}}/2\pi$ =160 kHz.

As described above, we at first define the parameters A_0, σ, K_h and K_l for two clearly non-equivalent positions of the methyl group of acetone molecules in NaX (altogether 8 parameters). In addition, three parameters A_0, σ and the pre-exponential factor, are needed to describe the correlation time of the acetone rotation. The methyl activation energy is defined by $A = A_0 + j\Delta A$, the quantities A_{r}, ω_{bt}, ω_{rt} and ω_{t} are obtained as described above and in [12], the correlation time is calculated from Eq. (1), and finally the individual relaxation rates R_{Ain} and R_{Ein} from Eqs. (3) (with modifications explained above). The relaxation rate R_{mol} is obtained from the modified equation (2). The comparison of the total relaxation rates $R_{\mathrm{Ain}} + R_{\mathrm{mol}}$ and $R_{\mathrm{Ein}} + R_{\mathrm{mol}}$ with the limiting values L_{fm} and L_{ms} defines, to which component this total relaxation rate contributes. When all the important points of the activation energy distributions (the weight must be sufficiently larger than zero for being important) have been taken into account, we obtain numerical values for the three relaxation rates R_{f}, R_{m} and R_{s} and the corresponding weights. These are compared with the experimental rates and weights, and then some or all of the mentioned 11 parameters are adjusted and new numerical, hopefully better, values obtained for R_{f}, R_{m} and R_{s} and the weights. This procedure is repeated so many times that the best possible agreement is obtained between experimental and theoretical results.

It was mentioned above that if the acetone motion makes the quadrupole coupling completely time-dependent, then Eq. (2), with the multiplier $\omega_{\mathrm{Q}}^2/15$ replaced by $\omega_{\mathrm{Q}}^2/120$, can be used for calculating the contribution of the acetone motion to the deuteron relaxation. In NaX and NaY the deuteron spectra show that the fast oscillations of acetone about its Z axis (augmented at higher temperatures by oscillations about the Y and X axes) dominate the acetone motion over a wide temperature range. If the jump angle about the Z axis (the twofold axis of the acetone molecule) were 180º, the multiplier would be $\omega_{\mathrm{Q}}^2/180$. But the angles are much smaller and therefore also the relaxation effectiveness must be smaller. It turned out that the multiplier $\omega_{\mathrm{Q}}^2/360$ was the best choice. Actually acetone motion is slower than methyl rotation and thus does not contribute much to the total relaxation rate until above 90 K. More reliable information about it is obtained from the experiments between 90 K and 170 K. There the relaxation curves could be described quite accurately with two exponentials. Our method was modified for that case. The high-temperature end of our results in Figs. 6 and 7 shows both the experimental and theoretical results for these temperatures.

When comparing our simulated results with experiment we realise that both the calculated relaxation rate and weight of the fast component agree rather well with experimental data. Also the corresponding quantities of the intermediate component agree satisfactorily. In addition, the rates and weights for temperatures between 80 and 170 K agree with experimental results. The calculated relaxation rate of the slow component agrees reasonably with experiment below 35 K but exceeds it somewhat at higher temperatures. Also the corresponding weight agrees with experiment only at few discrete temperatures. Table 1 gives the best-fit parameters for the methyl and acetone motions.

Our simulations require altogether 12 parameters, when also the multiplier of Eq. (2) is taken as a parameter. However, we have also 8 independent data sets: 3 relaxation

curves for temperatures 20 K − 80 K, 2 relaxation curves for 80 K − 170 K, 2 weights for 20 K − 80 K, and finally 1 weight for 80 K − 170 K. These all should be explained by the model depending on 12 parameters. Thus there are more data sets per parameter than in the conventional case of exponential relaxation, where the correlation time is determined by the activation energy of the Arrhenius equation and the pre-exponential factor.

We tried if a reasonable agreement between experiment and calculations could be obtained by assuming both the methyl groups of the acetone molecule practically equivalent. Then only one set of parameters A_0, σ, K_h and K_l is needed to describe the methyl rotation. It turned out that the best fits obtained this way were not as satisfactory as those shown in Figs. 6 and 7. Larger deviations occurred especially in the weights of the intermediate and slow components.

5.3. Calculations and discussion for NaY

First numerical calculations were done as described for NaX by assuming two clearly non-equivalent positions, with equal populations, for methyl groups. In the two-exponential regime between 140 K and 160 K the relaxation rates and weights agree rather well with experiment. Also in the three-exponential regime the fast-component quantities R_f and w_f are acceptable. But the discrepancies start with the intermediate component and are largest with the slow component. Therefore two non-equivalent methyl positions with equal populations w_n = ½ do not provide an acceptable interpretation.

Figures 8 and 9 show that about 1/6 of the deuterons in NaY relax practically at a constant rate equal to 0.1 1/s below 70 K. It is reasonable to believe that this rate is determined by spin diffusion, related to the magnetic dipolar interaction between the deuterons of the two methyl groups in the acetone molecule. The shortest deuteron−deuteron intermethyl distance is consistent with this claim. Therefore, no individual relaxation rate $R_{Ein} + R_{mol} + R_{spin\ diffusion}$ or $R_{Ain} + R_{mol} + R_{spin\ diffusion}$ can be smaller than 0.1 1/s. We still assume two clearly non-equivalent positions for the methyl groups, corresponding to clearly different A_0 and σ values, but now the corresponding occupations are taken equal to 5/6 and 1/6. By using a very broad activation-energy distribution for methyl rotation in the more populated position, we obtained remarkably improved fits represented by continuous curves in Figs. 8 and 9, corresponding to the parameters given in Table 1. The difficulties concerning the relaxation rate and weight of the slowly relaxing component are practically removed. The largest deviations occur in the weight of the intermediate and slow component below 50 K.

The acetone molecules containing faster rotating methyl groups were assumed to oscillate and thus contribute to R_{mol}. There may also be an oscillatory contribution to the relaxation rate of the slowly reorienting methyl groups, but it is masked by the dominant effect of the methyl rotation.

We tried also a model in which there are three clearly non-equivalent methyl positions, the relative occupations being roughly 2/12, 5/12 and 5/12, respectively, for the methyl groups reorienting at slow, intermediate and fast frequencies. The majority of the relaxation rates and weights remained practically intact, but clear improvements were obtained in the weight of the intermediate and slow component below 50 K. The improved fits are shown by broken curves in Fig. 9 and the corresponding parameters in Table 1. It is worth noticing that the two activation energy distributions of these fits, with the equal w_n occupations 5/12, cover practically the same energies as the rather broad distribution corresponding to 5/6 (83 %) of the deuterons in the fit represented by

continuous curves in Figs. 8 and 9. This seems to suggest that the true distribution is flatter than a Gaussian distribution and is therefore described more successfully by two Gaussians. Thus a very satisfactory fit is finally obtained, but at the expense of introducing three additional motional parameters and one population parameter.

We varied the w_n occupations to some extent and found that for example the populations 0.17, 0.33 and 0.50 lead practically to equally good fits, with small deviations in the low temperature weights w_m and w_s. Furthermore, the occupation weight 0.17 agrees reasonably well with the combined contribution of the Pake (rigid) doublets, which decreases through 17 % near 80 K (Fig. 5).

Actually the slowest component between 65 K and 120 K, with the weight 17 %, transforms with rising temperature to the fast-relaxing component above T_S, which was also observed to have the weight 17 %. On the other hand, the fast and intermediate components combine to one slower component in the two-exponential region above 140 K. By using the same parameters as in the three-component region, the relaxation rate of this slow component can be extrapolated up to 270 K (clearly higher than T_S), in excellent agreement with the relaxation data for the dominant component there [10]. This supports the applicability of the present procedure.

It can be derived from the calculations of Clough et al. [27] that normally the multiplying factors K_h and K_l in Eq. (1) do not differ very much from 1. For 1/6 of the deuterons in NaY we had to use for these factors very small values 0.001 and 0, respectively (see Table 1). Therefore, these deuterons do not seem to behave like "normal" methyl deuterons. Furthermore, their correlation time around T_S seems to shorten faster than that given by the activation energy in Table 1. These features may indicate that the bonds which make the corresponding methyl groups practically rigid below 70 K, are breaking above this temperature and especially near T_S, leading to rather freely rotating methyl groups at higher temperatures. This is also consistent with the claim that the acetone molecules at these high temperatures are bonded only to Na atoms via oxygen, which allows torsional oscillations about the twofold axis, in perfect agreement with the spectral results.

The motional parameters of Table 1 can be used to calculate the relative number of methyl groups with the tunnelling frequency larger than 1 MHz. This portion at 20 K and below is about 50 %, in a good agreement with the spectral result.

6. Conclusion

We have applied the rather recently introduced method [11, 12] for explaining the non-exponential deuteron relaxation of methyl groups of acetone molecules in zeolites NaX and NaY. Our starting point here is the assumption that there are essentially two kinds of non-equivalent methyl positions with clearly different mean activation energies A_0, but in each position there is a distribution of activation energies described by the width σ. The Mathieu equation together with some parameters enable then the calculation of the CD_3 rotational correlation time and the deuteron relaxation rate. The model was improved in [12] to take into account the effect of the tunnel frequency ω_t and the fact that at low temperatures the effective activation energy decreases. In the present study we calculated the higher limit for the magnetization growth via so-called level-crossing transitions. The success of the improved model is rather good with our present samples NaX and NaY containing deuterated acetone molecules, the major part of the calculated quantities fall within the error limits of our experiments.

The method itself is complicated and depends on several approximations, which makes it difficult to find out, what would be the most effective further improvement. One problem is that our calculations use the initial relaxation rates R_{Ain} and R_{Ein} to describe the growth of each component of the non-exponential relaxation, although in principle somewhat smaller "average" rates would give a better fit. This error could be corrected for in principle, but in practice it would lead to a huge increase in the computing time. The calculated relaxation rate for the intermediate component of NaY, which is consistently somewhat larger than the observed one, is believed to derive from that. Another possibility, which would reduce the mentioned deviation, is the use of somewhat smaller limiting values instead of $L_{\mathrm{fm}} = \sqrt{R_{\mathrm{f}} R_{\mathrm{m}}}$ and L_{ms}. An additional question is how well the activation energy distributions follow the Gaussian distribution. There is also some scatter in the experimental rates and weights when three exponentials are fitted to the relaxation curves. In any case the discussed method is the only one so far, which can be applied when the methyl tunnelling frequencies are near the resonance frequency. It can also be used when there are methyl (or other) groups in two or more distinctly non-equivalent positions. Furthermore, small discrepancies between experimental and theoretical results cause only small errors in the activation energies as far as the experimental and theoretical data show the same temperature dependence.

Acknowledgements

We thank Dr Grzegorz Stoch for participation in some measurements and Dr Kinga Góra-Marek for preparation of samples. Financial support from Jenny and Antti Wihuri Foundation is acknowledged. This study was a part of the project generously financed by the National Science Centre, Poland, grant No. N202 127939 during 2010 − 2014.

References

[1] J.S. Blicharski, Z.T. Lalowicz, W. Sobol, J. Phys. C: Solid State Phys. 11 (1978)4187–4200.
[2] Z.T. Lalowicz, U. Werner, W. Müller-Warmuth, Z. Naturforsch. 43a (1988) 219–227.
[3] A. Detken, P. Focke, H. Zimmermann, U. Haeberlen, Z. Olejniczak, Z.T. Lalowicz, Z. Naturforsch. 50a (1995) 95–116.
[4] D. van der Putten, N.J. Trappeniers, Physica A 129 (1985) 302–326.
[5] L.P. Ingman, E. Koivula, Z.T. Lalowicz, M. Punkkinen, E.E. Ylinen, Z. Phys. B – Condensed Matter 66 (1987) 363–373.
[6] L.P. Ingman, E. Koivula, M. Punkkinen, E.E. Ylinen, Z.T. Lalowicz, Physica B 162 (1990) 281–292.
[7] G. Diezemann, H. Sillescu, D. van der Putten, Z. Phys. B – Condensed Matter 83 (1991) 245−257.
[8] G. Diezemann, Appl. Magn. Reson. 17 (1999) 345–366.
[9] G. Buntkowsky, H. Breitzke, A. Adamczyk, F. Roelofs, T. Emmler, E. Gedat, B. Grünberg, Y. Xu, H.-H. Limbach, I. Shenderovich, A. Vyalikh. G. Findenegg, Phys. Chem. Chem. Phys. 9 (2007) 4843–4853.
[10] Z.T. Lalowicz, A. Birczyński, A. Krzyżak, J. Phys. Chem. C 121 (2017) 26472−26482.
[11] G. Stoch, E.E. Ylinen, A. Birczyński, Z.T. Lalowicz, K. Góra-Marek, M. Punkkinen,

Solid State Nucl. Magn. Reson. 49−50 (2013) 33−41.
[12] E.E. Ylinen, M. Punkkinen, A. Birczyński, Z.T. Lalowicz, Solid State Nucl. Magn. Reson. 71 (2015) 19−29.
[13] E. Rössler, M. Taupitz, K. Börner, M. Schulz, H.-M. Vieth, J. Chem. Phys. 92 (1990) 5847–5855.
[14] C. Schmidt, K.J. Kuhn, H.W. Spiess, Progr. Colloid & Polymer Sci. 71 (1985) 71–76.
[15] E. Rössler, M. Taupitz, H.-M. Vieth, J. Phys. Chem. 94 (1990) 6879–6884.
[16] P.M. Cereghetti, R. Kind, J.S. Higgins, J. Chem. Phys. 121 (2004) 8068–8078.
[17] I. Roggatz, E. Rössler, M. Taupitz, R. Richert, J. Phys. Chem. 100 (1996) 12193−12198.
[18] L. Vugmeyster, D. Ostrovsky, T. Villafranca, J. Sharp, W. Xu, A.S. Lipton, G.L. Hoatson, R.L. Vold, J. Phys. Chem. B 119 (2015) 14892−14904.
[19] D.H. Barich, J.B. Nicholas, T. Xu, J.F. Haw, J. Am. Chem. Soc. 120 (1998) 12342−12350.
[20] H. Fang, A. Zheng, Y. Chu, F. Deng, J. Phys. Chem. C 114 (2010) 12711−12718.
[21] T. Xu, E.J. Munson, J.F. Haw, J. Am. Chem. Soc. 116 (1994) 1962−1972.
[22] A.I. Biaglow, R.J. Gorte, D. White, J. Phys. Chem. 97 (1993) 7135−7137.
[23] J. Haupt, Z. Naturforsch. 26a (1971) 1578–1589.
[24] W. Müller-Warmuth, R. Schüler, M. Prager, A. Kollmar, J. Chem. Phys. 69 (1978) 2382–2392.
[25] J.L. Skinner, H.P. Trommsdorff, J. Chem. Phys. 89 (1999) 345–366.
[26] E.O. Stejskal, H.S. Gutowsky, J. Chem. Phys. 28 (1955) 388–396.
[27] S. Clough, A. Heidemann, A.J. Horsewill, J.D. Lewis, N.J. Paley, J. Phys. C: Solid State Phys. 15 (1982) 2495–2508.
[28] S. Szymanski, J. Chem. Phys. 111 (1999) 288–299.
[29] M. Kankaanpää, M. Punkkinen, E.E. Ylinen, Mol. Phys. 100 (2002) 2877−2893.
[30] M. Bloom, J.H. Davis, M.I. Valic, Can. J. Phys. 58 (1980) 1510−1517.
[31] V. Macho, L. Brombacher, H.W. Spiess, Appl. Magn. Reson. 20 (2001) 405−432.
[32] K.A. Udachin, G.D. Enright, C.I. Ratcliffe, J.A. Ripmeester, ChemPhysChem 4 (2003) 1059− 1064.
[33] P.S. Sidhu, J. Bell, G.H. Penner, K.R. Jeffrey, Can. J. Chem. 73 (1995) 2196–2207.
[34] C.L. Angell, P.C. Schaffer, J. Phys. Chem. 70 (1966) 1413−1418.
[35] Z.T. Lalowicz, G. Stoch, A. Birczyński, M. Punkkinen, E.E. Ylinen, M. Krzystyniak, K. Góra-Marek, J. Datka, Solid State Nucl. Magn. Reson. 45–46 (2012) 66–74.

Table I
Motional parameters for methyl groups and acetone molecules in NaX and NaY zeolite

zeolite	methyl groups	two species		three species			Acetone molecules
NaX	occupation	1/2	1/2				
	A_0 (kJ/mol)	3.0	4.9				10.5
	σ (kJ/mol)	0.4	0.7				2.2
	K_h	4.0	4.0				
	K_l	0.3	0.3				
	τ_0 (10^{-14} s)						3.0
NaY	occupation	5/6	1/6	5/12	5/12	2/12	
	A_0 (kJ/mol)	5.2	8.2	4.3	7.0	7.8	10.0
	σ (kJ/mol)	1.4	1.8	0.6	1.0	1.7	1.7
	K_h	1.5	0.001	1.0	6.0	0.001	
	K_l	1.0	0	1.0	1.0	0	
	τ_0 (10^{-14} s)						1.0

Figure captions

Fig. 1. Deuteron NMR spectra of acetone-d_6 with internal rotation of methyl groups, performing consecutive torsional oscillations about three perpendicular symmetry axes of acetone molecule. See section 4 for details.

Fig. 2. Deuteron NMR spectra of acetone-d_6 in NaX at 100% loading.

Fig. 3. The relative contributions of spectral components of acetone-d_6 in NaX zeolite as the function of temperature: Pake doublet with C_Q = 105 kHz (filled circles), Pake doublet with C_Q = 170 kHz (open circles), component lt (open triangles), component mt (open diamonds), component ht (filled triangles), Gaussian component (crossed circles).

Fig. 4. Deuteron NMR spectra of acetone-d_6 in NaY at 100% loading.

Fig. 5. The relative contributions of spectral components of acetone-d_6 in NaY zeolite as the function of temperature: Pake doublet with C_Q = 107 kHz (filled circles), Pake doublet with C_Q = 177 kHz (open circles), tunnelling methyl groups (filled squares), component lt (open triangles), component mt (open diamonds), component ht (filled triangles), narrow Gaussian component (crossed circles) and broad Gaussian component (stars).

Fig. 6. The observed relaxation rates R_f, R_m and R_s as the function of temperature for acetone-d_6 in NaX. The continuous curves represent the best-fit simulated results.

Fig. 7. The experimental weights of the fast, intermediate and slow components of acetone-d_6 in NaX, together with the simulated weights.

Fig. 8. The observed relaxation rates R_f, R_m and R_s as the function of temperature for acetone-d_6 in NaY. The continuous curves represent the best-fit simulated results.

Fig. 9. The experimental weights of the fast, intermediate and slow components of acetone-d_6 in NaY, together with the simulated weights. The dashed curves show the simulated weights when three clearly non-equivalent methyl positions are used in the model (section 5.3).

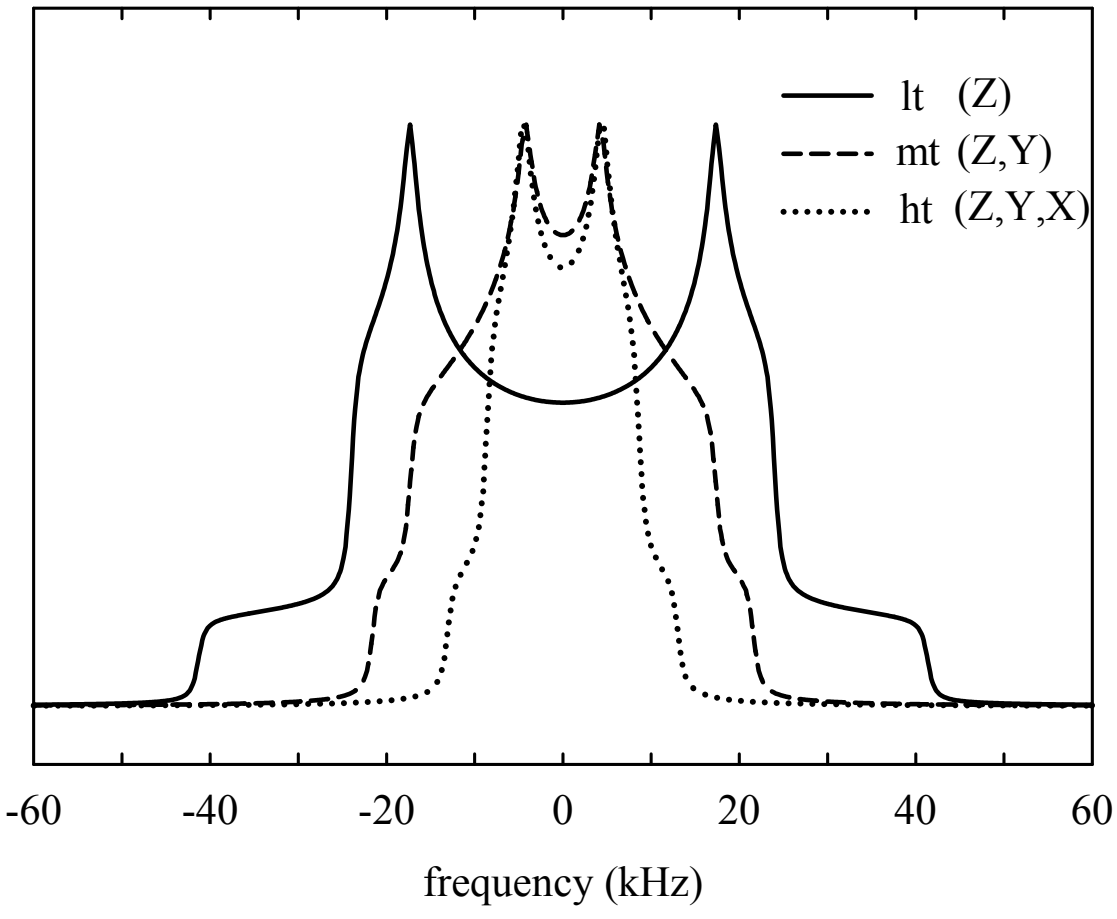

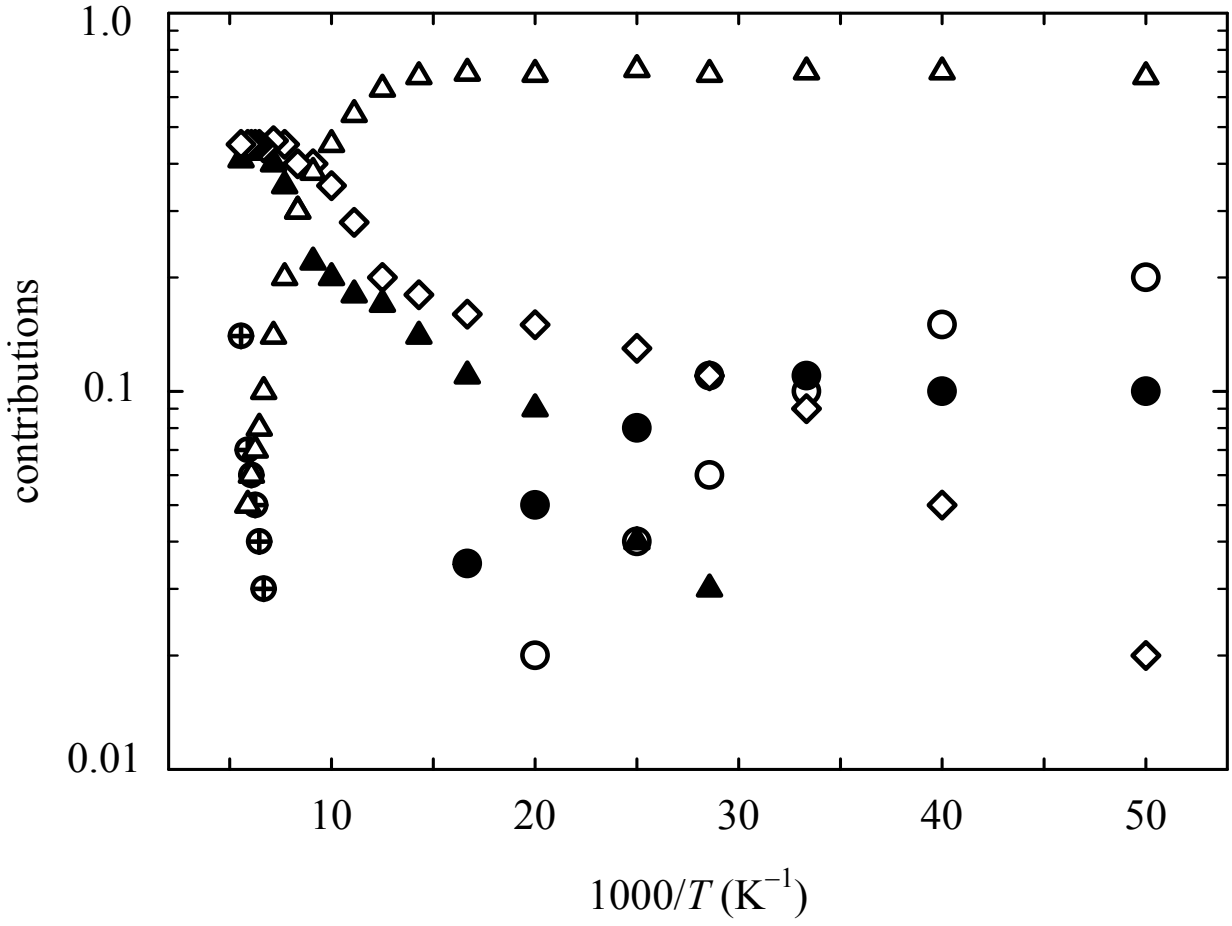

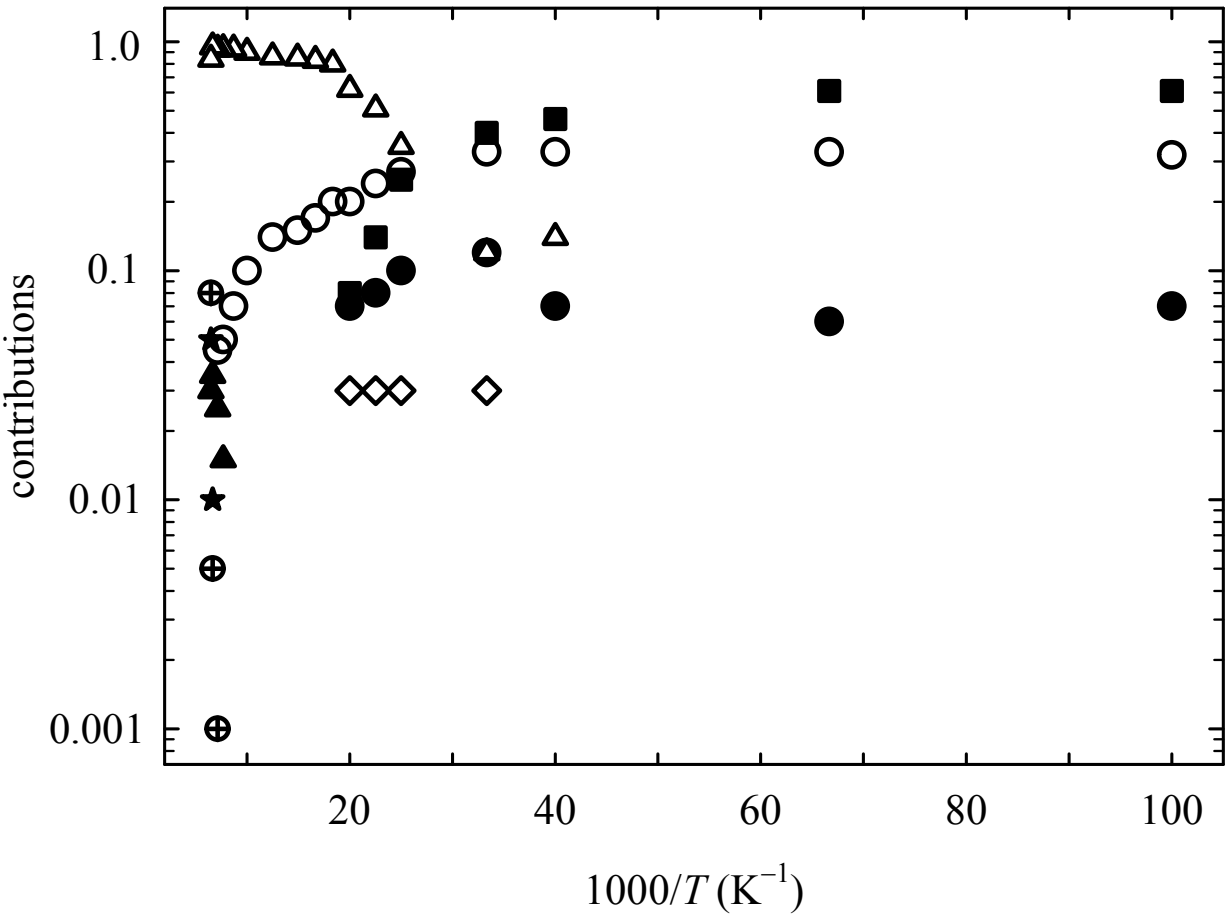

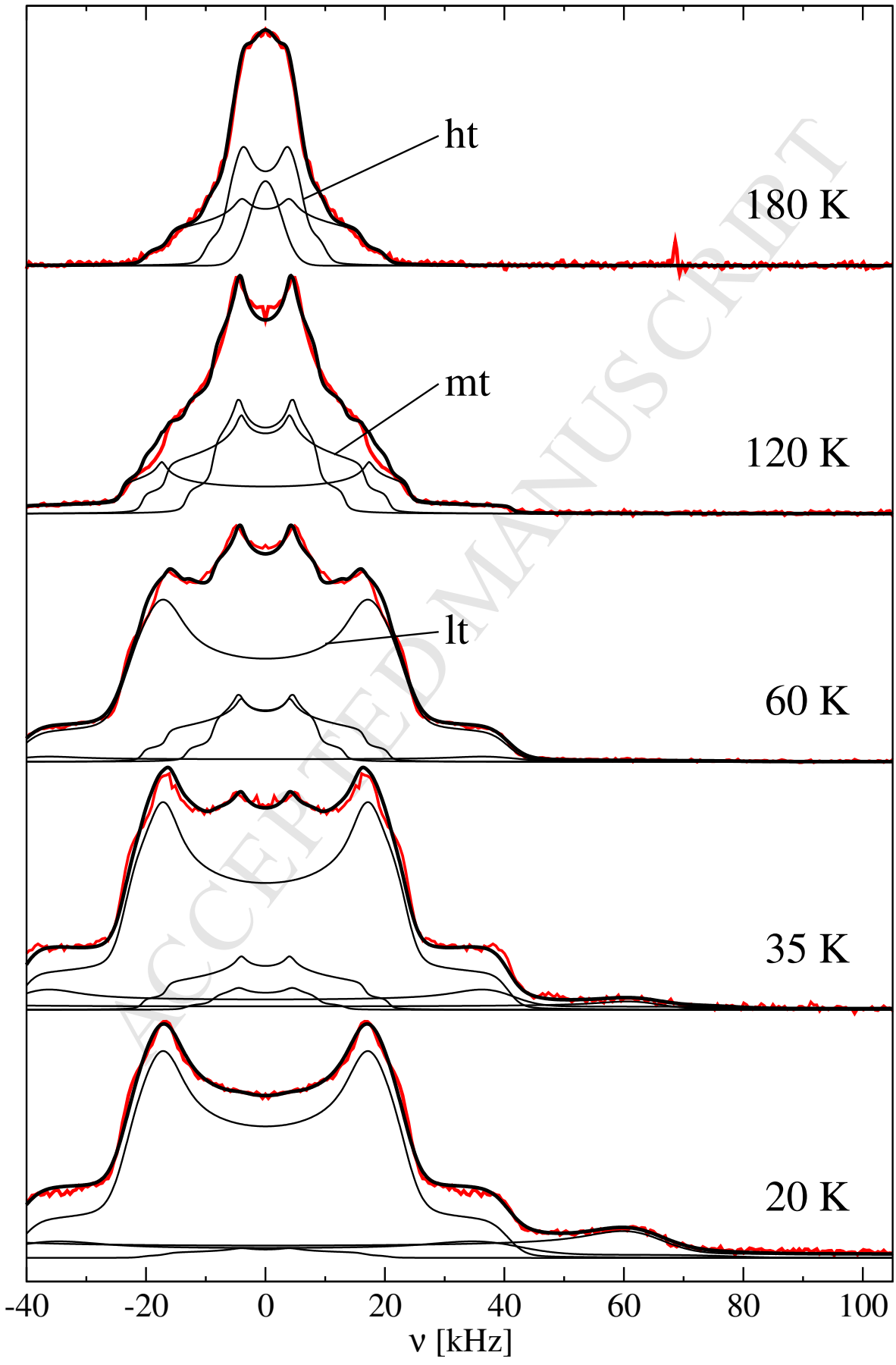

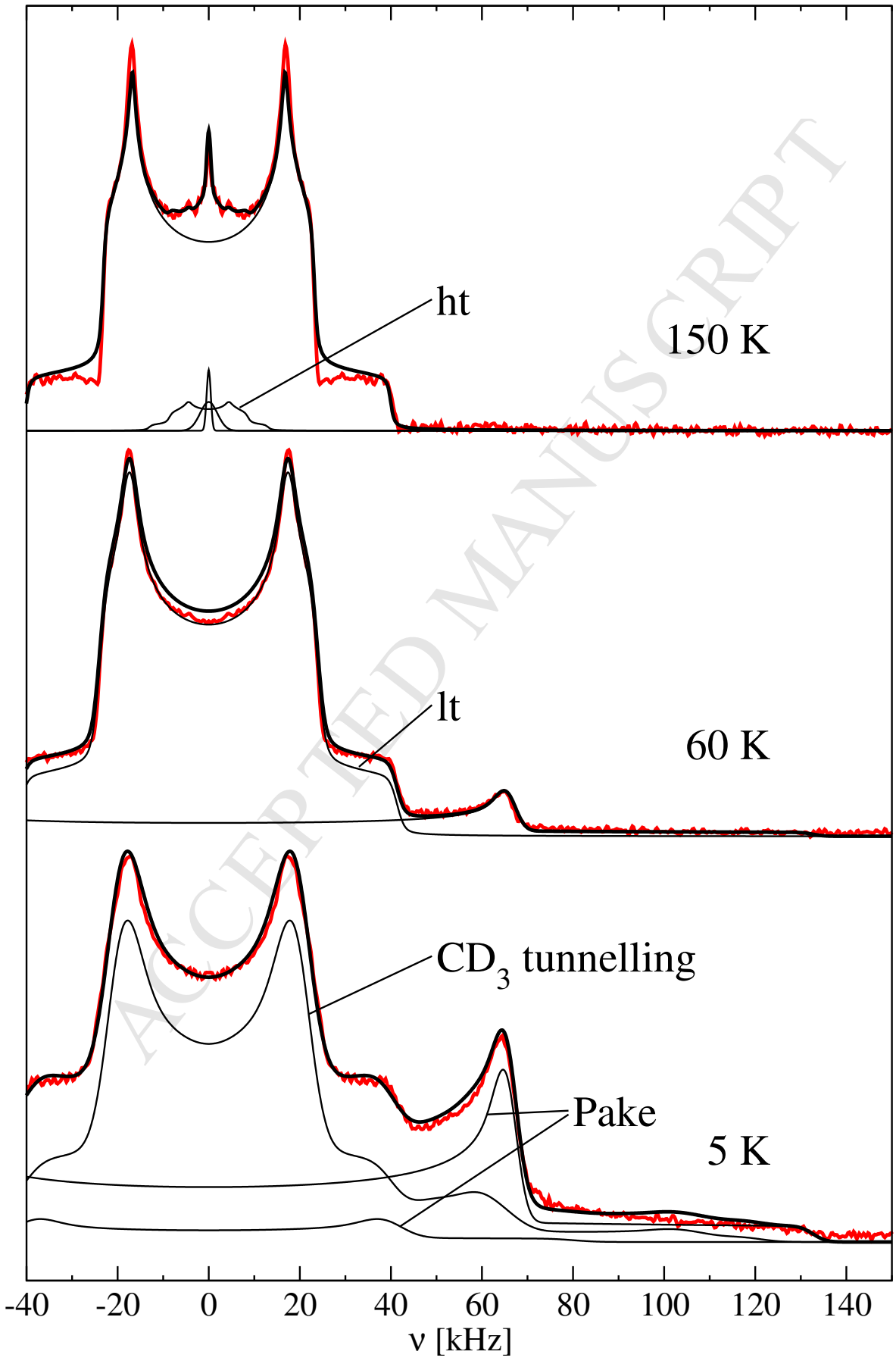

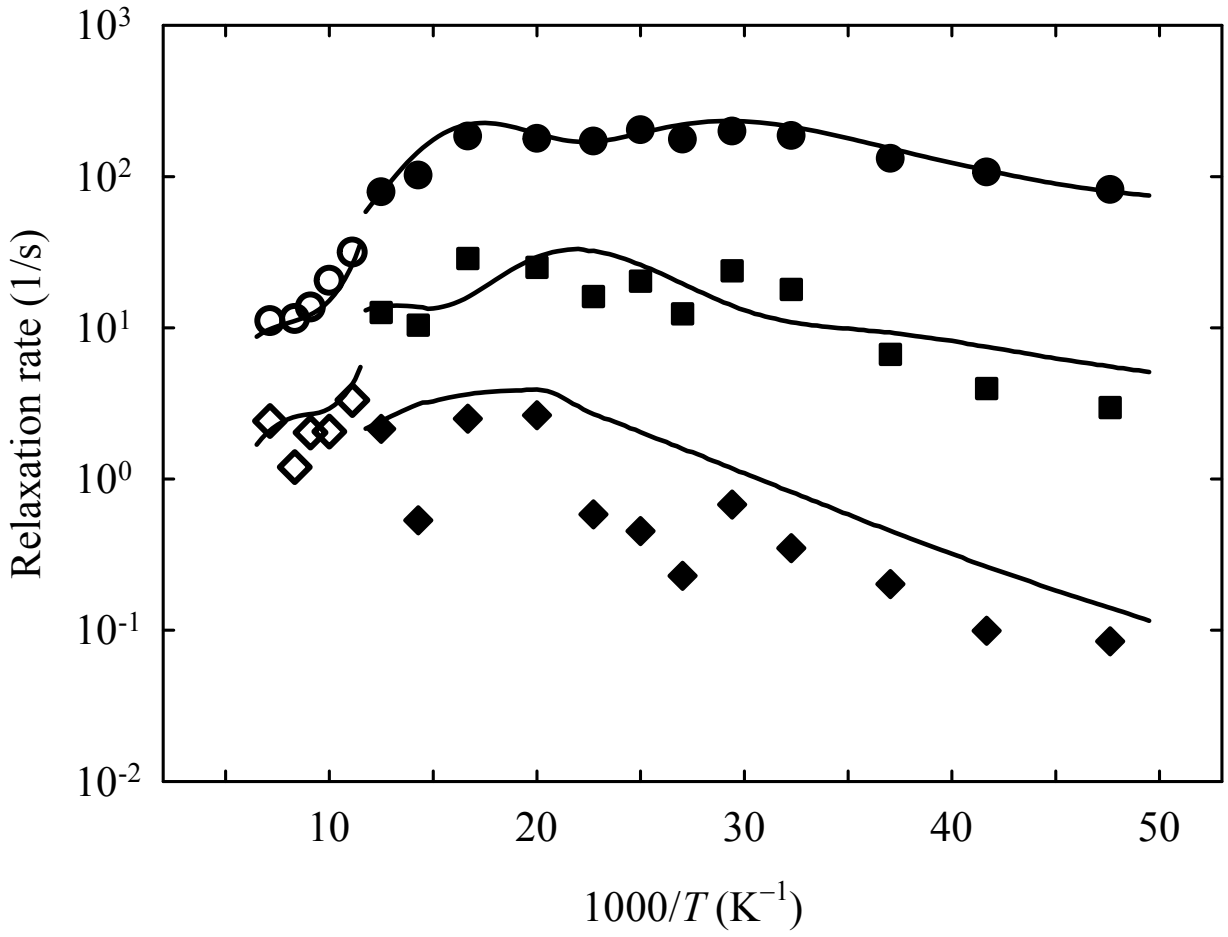
10^3
10^2
10^1
10^0
10^{-1}
10^{-2}
Relaxation rate (1/s)
10
20
30
40
50
1000/T (K^{-1})

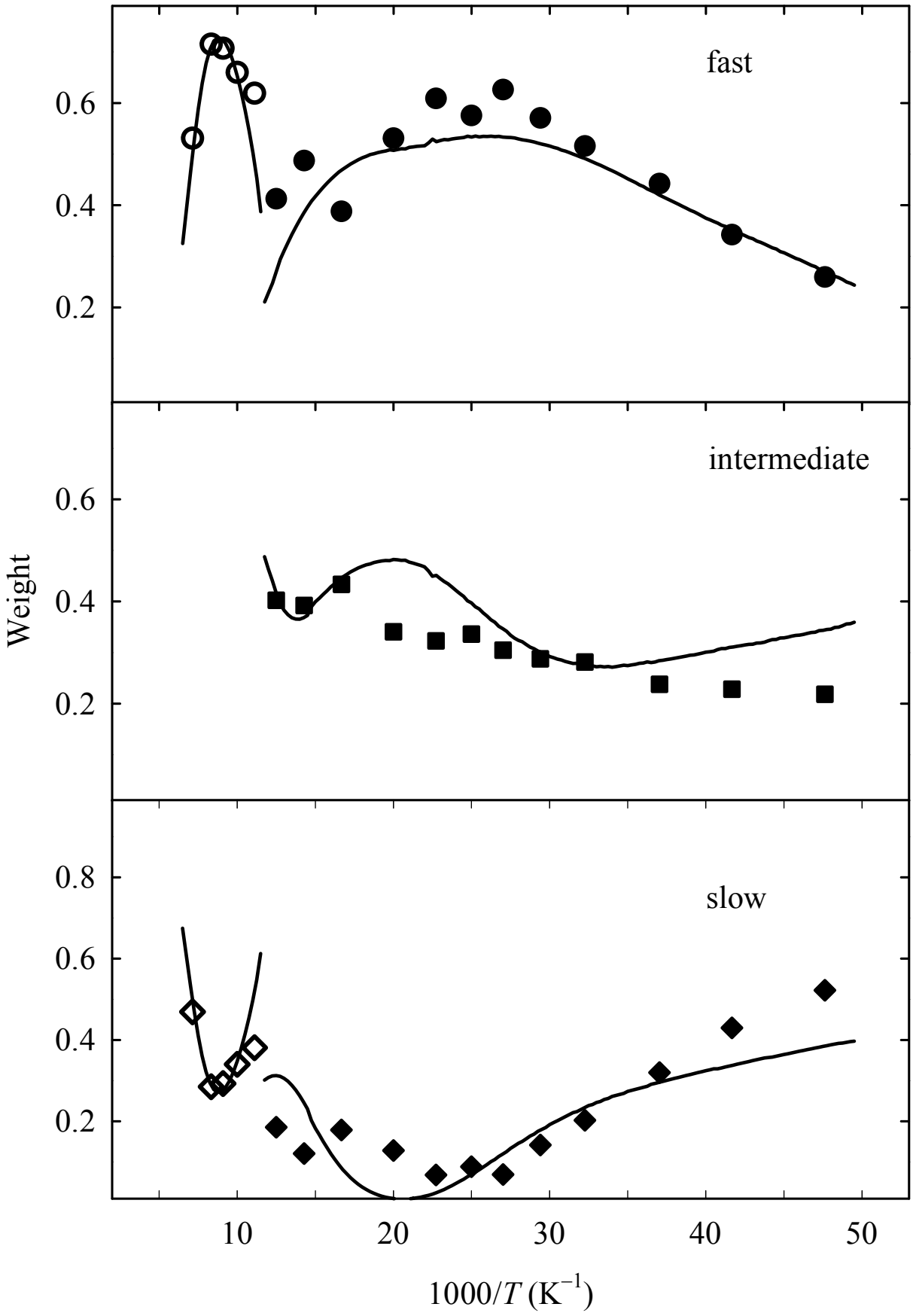
fast
intermediate
slow
Weight
0.2
0.4
0.6
0.8
10
20
30
40
50
1000/T (K^-1)

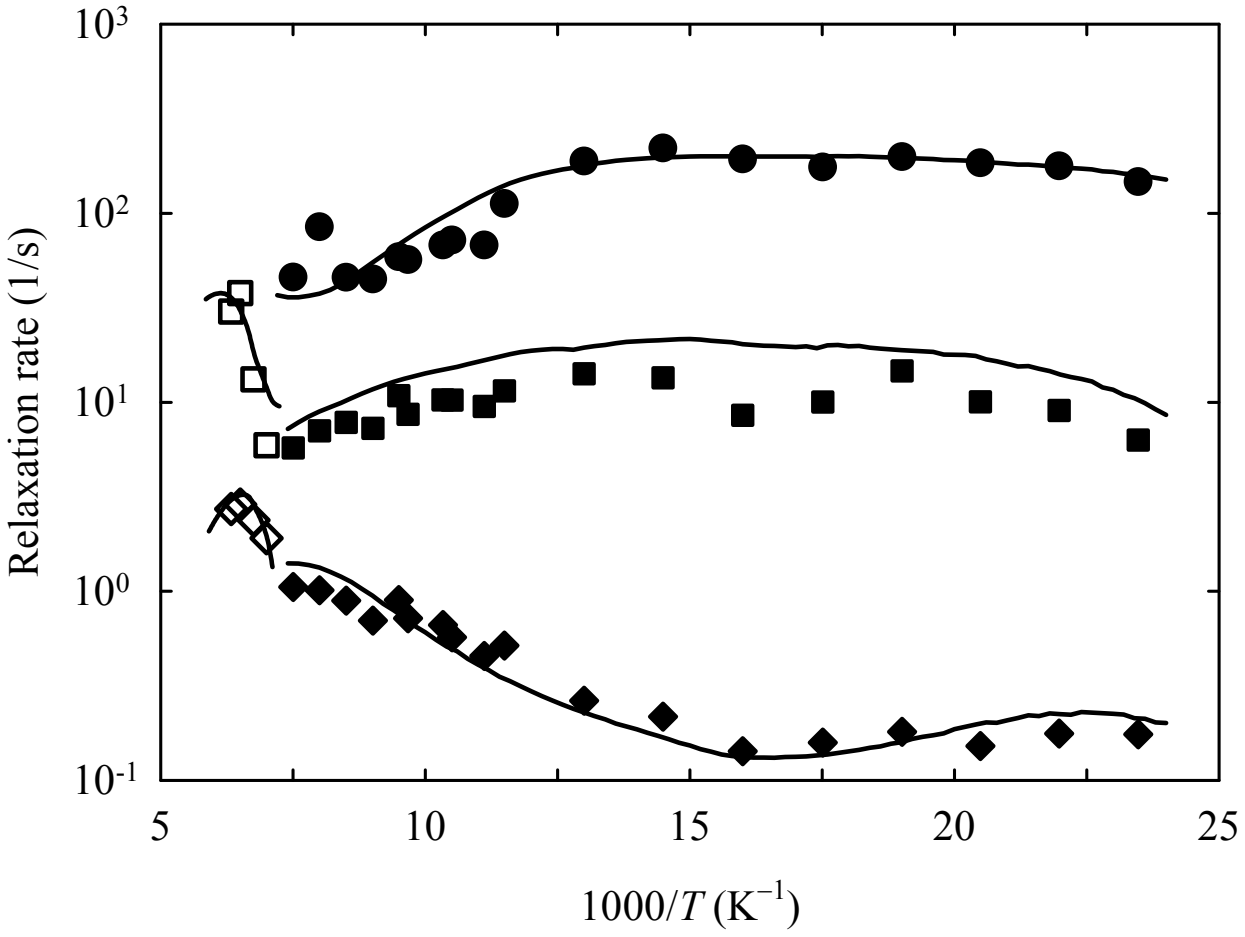

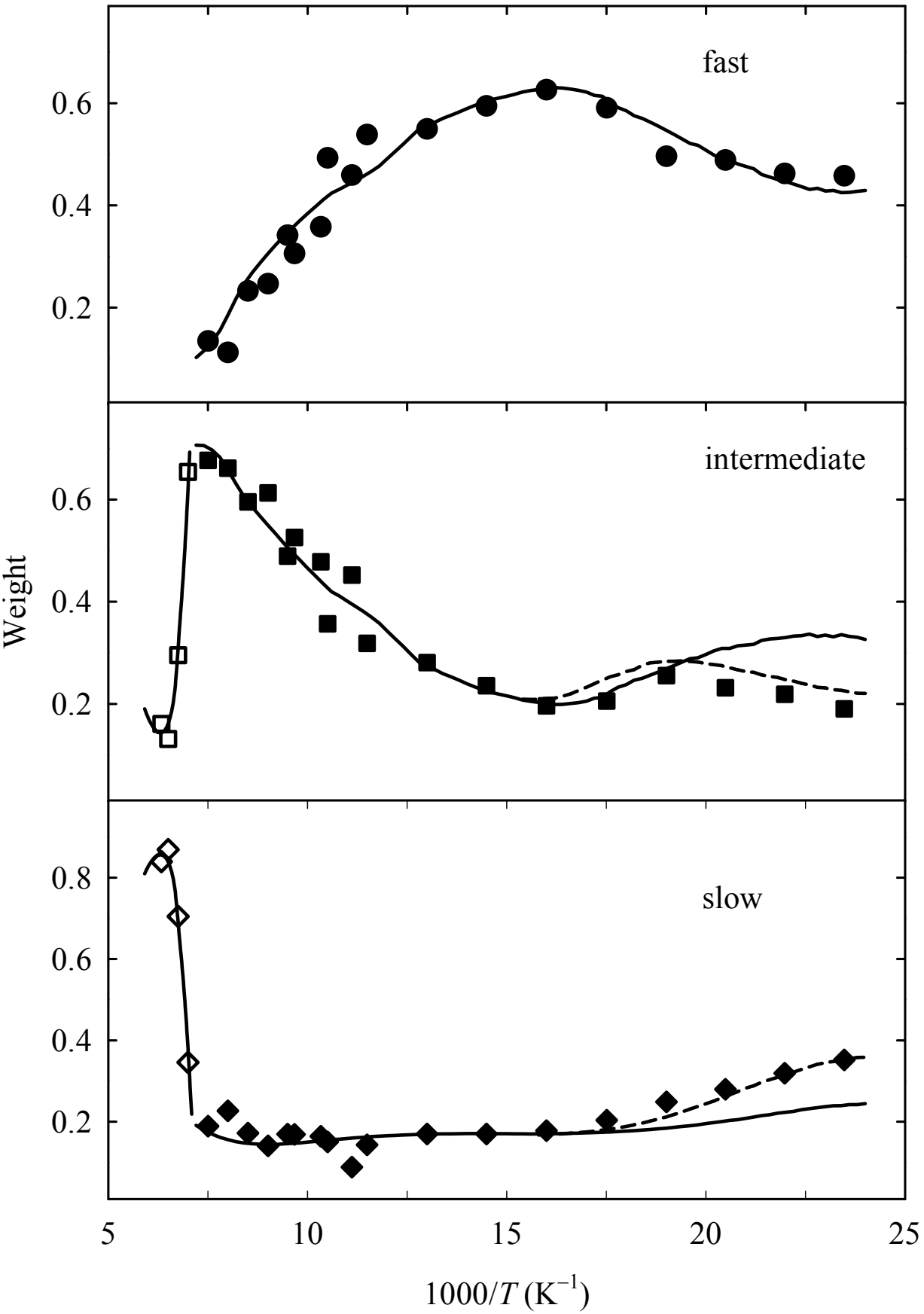
fast
intermediate
slow
Weight
0.2
0.4
0.6
0.8
5
10
15
20
25
1000/T (K−1)

- Non-exponential deuteron spin−lattice relaxation and activation energy distributions
- The effect of a large tunnel splitting and decreasing activation energy on relaxation
- Simulation of relaxation rates in a wide range of temperature
- Acetone in zeolites NaX(1.3) and NaY(2.4)
- Effects of methyl rotation and rotational jumps of acetone on deuteron spectra

Supplementary Material to the article:

Acetone mobility in zeolite cages with new features in the deuteron NMR spectra and relaxation

E.E. Ylinen, M. Punkkinen, A. Birczyński, Z.T. Lalowicz

Deuteron spin−lattice relaxation in CD_3 near the level-crossing conditions

Here we will figure out, to which extent the total deuteron magnetization M_Z of CD_3 groups relaxes via level-crossing transitions. For that purpose the starting functions have to be defined. We use the same spin−rotational functions as in the study [12] and its Supplemental Material. The spin functions are expressed utilizing symbols like $(10\bar{1})$, which means that the spin states of the three methyl deuterons u, v and w are m = 1, 0 and −1, respectively. We use the same spin functions as in Supplemental Material of [12].

$$
\begin{aligned}
&S_{A3} = (111)\\
&S_{A2} = (1/\sqrt{3})[(110) + (011) + (101)]\\
&S_{A1} = (1/\sqrt{3})[(11{-}1) + (-111) + (1{-}11)]\\
&S'_{A1} = (1/\sqrt{3})[(001) + (100) + (010)]\\
&S_{A0} = (1/\sqrt{6})[(1{-}10) + (-110) + (01{-}1) + (0{-}11) + (-101) + (10{-}1)]\\
&S'_{A0} = (1/\sqrt{6})[(1{-}10) - (-110) + (01{-}1) - (0{-}11) + (-101) - (10{-}1)]\\
&S''_{A0} = (000)\\
&S_{Ea2} = (1/\sqrt{3})[(110) + \varepsilon(011) + \varepsilon^*(101)]\\
&S_{Ea1} = (1/\sqrt{3})[(11{-}1) + \varepsilon(-111) + \varepsilon^*(1{-}11)]\\
&S'_{Ea1} = (1/\sqrt{3})[(001) + \varepsilon(100) + \varepsilon^*(010)]\\
&S_{Ea0} = (1/\sqrt{6})\{(1{-}10) + (-110) + \varepsilon[(01{-}1) + (0{-}11)] + \varepsilon^*[(-101) + (10{-}1)]\}\\
&S'_{Ea0} = (1/\sqrt{6})\{(1{-}10) - (-110) + \varepsilon[(01{-}1) - (0{-}11)] + \varepsilon^*[(-101) - (10{-}1)]\}
\end{aligned}
\qquad \text{(S1)}
$$

where $\varepsilon = \exp(i2\pi/3)$. The spin functions for the negative values of m are obtained from (S1) by interchanging 1 and −1. By interchanging ε and ε^* in S_{Eam} and S'_{Eam} we obtain the corresponding S_{Ebm} and S'_{Ebm} functions.

Some of these functions are also eigenfunctions of the total spin, namely S_{Am} (m = ±3, ±2), S'_{A0}, S_{Ea0}, S'_{Ea0}, S_{Eb0} and S'_{Eb0}. However, the functions (S1) are simultaneous eigenfunctions of the rotational, Zeeman, and secular quadrupole Hamiltonians as far as $\omega_Q\tau < 1$ [3]. Therefore, they are just proper functions for relaxation considerations. Furthermore, as simple combinations they are easy to use. At low temperatures corresponding to $\omega_Q\tau > 1$ the non-secular quadrupole coupling mixes some of these functions. The resulting changes in the degree of the fast magnetization recovery are expected to be insignificant.

The threefold rotational symmetry of the methyl group requires that the A, E^a and E^b species spin function has to be multiplied by the A, E^b and E^a species rotational function, respectively, to obtain an A species spin−rotational function. The obtained product functions are labelled with the indices of the spin functions.

The rotational eigenfunctions were calculated from the Mathieu equation and the results were used in the evaluation of the correlation time (1). However, for the following considerations of the fast magnetization recovery the accurate values of the rotational functions are not needed.

The matrix elements of the quadrupole interaction between these eigenstates, and also the corresponding transition rates, were calculated in Supplemental Material of [12]. There are altogether 14 different transition rates but only 4 of them are related to level crossings

$$R_{\mathrm{ta}-1} = \frac{9}{32}\omega_{\mathrm{Q}}^2\left|\mathrm{B}_{\mathrm{Ea}}^{(-1)}\right|^2 \mathrm{J}(\tau,\omega_{\mathrm{t}} - \omega_0)$$
$$R_{\mathrm{ta}-2} = \frac{9}{64}\omega_{\mathrm{Q}}^2\left|\mathrm{B}_{\mathrm{Ea}}^{(-2)}\right|^2 \mathrm{J}(\tau,\omega_{\mathrm{t}} - 2\omega_0) \qquad \text{(S2)}$$

the remaining 2 rates $R_{\mathrm{tb}-1}$ and $R_{\mathrm{tb}-2}$ being obtainable from $R_{\mathrm{ta}-1}$ and $R_{\mathrm{ta}-2}$ by replacing $\mathrm{B}_{\mathrm{Ea}}^{(-\mathrm{m})}$ by $\mathrm{B}_{\mathrm{Eb}}^{(-\mathrm{m})}$. The correlation time τ is equal to the inverse of $\mathrm{k_t}$, the damping rate of the tunnelling coherence [28]. The orientation dependence of these rates is obtained from Table 3 of [29]

$$\left|\mathrm{B}_{\mathrm{Ea,\,Eb}}^{(-1)}\right|^2 = \frac{2}{81}\left[3 \mp 6\mathrm{c} - 3\mathrm{c}^2 \pm 8\mathrm{c}^3 + 2\mathrm{c}^4 + 2\sqrt{2}(\mathrm{a}^2 - 3\mathrm{b}^2)(2\mathrm{ac}\mp\mathrm{a})\right]$$
$$\left|\mathrm{B}_{\mathrm{Ea,\,Eb}}^{(-2)}\right|^2 = \frac{4}{81}\left[3 + 6\mathrm{c}^2 \mp 8\mathrm{c}^3 - \mathrm{c}^4 - 2\sqrt{2}(\mathrm{a}^2 - 3\mathrm{b}^2)(\mathrm{ac} \mp \mathrm{a})\right] \qquad \text{(S3)}$$

where the upper signs are for $\mathrm{B}_{\mathrm{Ea}}^{(-\mathrm{m})}$ and lower signs for $\mathrm{B}_{\mathrm{Eb}}^{(-\mathrm{m})}$. The direction cosines are $\mathrm{a} = \sin\theta\cos\phi$, $\mathrm{b} = \sin\theta\sin\phi$ and $\mathrm{c} = \cos\theta$, where the azimuth and phase angles θ and ϕ define the direction of the external magnetic field in the CD_3 fixed coordinate system, with the z axis parallel to the methyl axis and one of the C−D bonds lying in the xz plane. It is worth noticing that both $R_{\mathrm{tb}-1}$ and $R_{\mathrm{ta}-2}$ vanish when c = 1 (eg. the magnetic field is parallel to the methyl axis).

Let us consider the situation that the tunnel frequency ω_{t} equals $2\omega_0$. Fig. 1S describes the energy levels AM and $\mathrm{E^aM}$ for that situation when the quadrupolar shifts are ignored. Of course the $\mathrm{E^bM}$ energies are equal to the $\mathrm{E^aM}$ energies although they are not mentioned explicitly. The level A”0 is not shown because it is not connected to other levels via the level-crossing transitions in the present case. The inclined lines define the population of each level at thermal equilibrium according to the Boltzmann distribution

$$\mathrm{N_{EaM}} = \mathrm{N_{EbM}} = \mathrm{P}\exp[-\hbar(\omega_{\mathrm{t}} - \mathrm{M}\omega_0)/\mathrm{k}T] = \mathrm{P}(1 - 2\delta + \mathrm{M}\delta) \text{ and } \mathrm{N_{AM}} = \mathrm{P}(1 + \mathrm{M}\delta). \qquad \text{(S4)}$$

Here P is the normalizing constant and $\delta = \hbar\omega_0/\mathrm{k}T = \hbar\omega_{\mathrm{t}}/2\mathrm{k}T$.

Immediately after the saturation of the deuteron magnetization the populations are $\mathrm{N_{AM}} = \mathrm{P}$ and $\mathrm{N_{EaM}} = \mathrm{N_{EbM}} = \mathrm{P}(1-2\delta)$ and they are described by the vertical broken lines. Simultaneously the relaxation starts and it is dominated by the level-crossing rates $R_{\mathrm{ta}-2}$ and $R_{\mathrm{tb}-2}$; actually we ignore totally the remaining rates. The AM and $\mathrm{E^aM’}$ levels are connected only by $R_{\mathrm{ta}-2} = R$; the latter symbol being used for brevity. R is drawn between all the states, which it connects (see Table 1 of Supplemental Material of [12]). In addition, a dotted line is drawn between the states $\mathrm{E^a}2$ and A’0 to show that R connects also these states. Furthermore, the rate $R_{\mathrm{tb}-2}$ connects the corresponding $\mathrm{E^bM’}$ levels to AM levels. Thus for example the levels $\mathrm{E^a}0$, $\mathrm{E^b}0$, A−2, $\mathrm{E^a’}0$ and $\mathrm{E^b’}0$ are connected and the mentioned rates equalize their populations fast. Immediately after the saturation the sum of

these 5 populations is P(5 − 8δ). After the fast equalization the populations become $N_{Ea0} = N_{Eb0} = N_{A-2} = N_{Ea'0} = N_{Eb'0} = P(1 - 8\delta/5)$. Similarly the other populations can be calculated. The total deuteron magnetization is

$$M_z/\gamma\hbar = 3(N_{A3} - N_{A-3}) + 2(N_{A2} - N_{A-2}) + (N_{A1} - N_{A-1}) + (N_{A'1} - N_{A'-1}) + 2(N_{Ea2} - N_{Ea-2}) + 2(N_{Eb2} - N_{Eb-2}) + (N_{Ea1} - N_{Ea-1}) + (N_{Eb1} - N_{Eb-1}) + (N_{Ea'1} - N_{Ea'-1}) + (N_{Eb'1} - N_{Eb'-1}). \quad \text{(S5)}$$

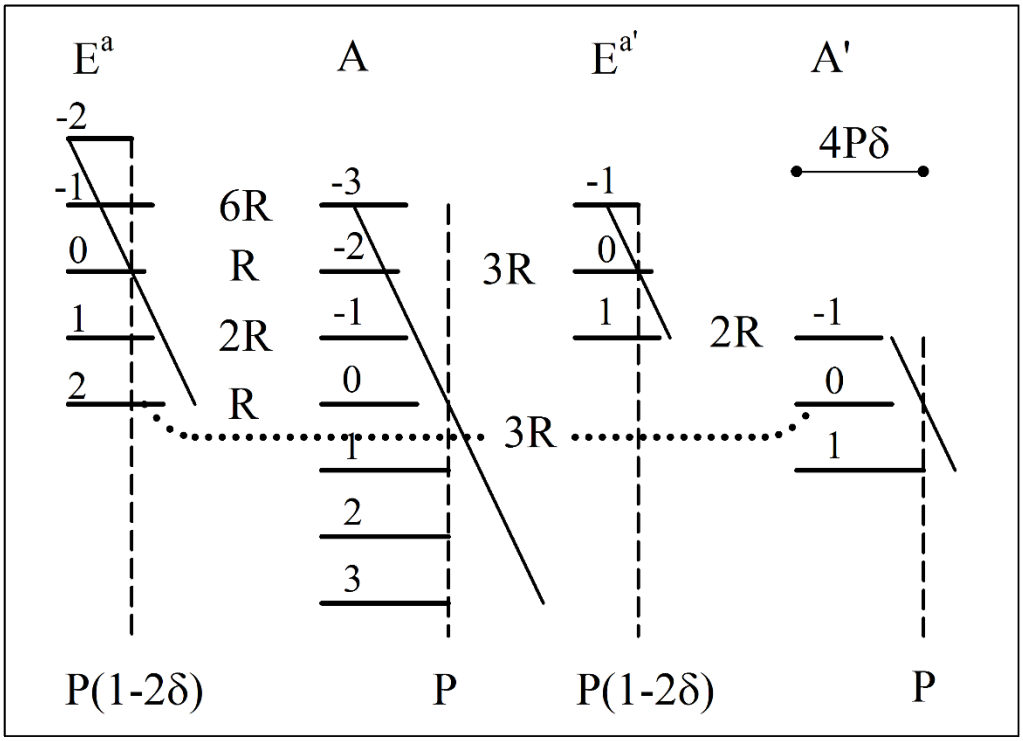

Fig. 1S. Energy levels Am, A′m, E^am, $E^{a\prime}$m and the fast transition rates proportional to $R = R_{ta-2}$ for $\omega_t = 2\omega_0$ and $\delta = \hbar\omega_0/kT$. The levels E^bm, $E^{b\prime}$m are equal to the corresponding E^a levels. The inclined lines and the vertical broken lines describe the populations at thermal equilibrium and just after the saturation, respectively. The line lengths represent the populations after the completion of the fast relaxation. The level A′′0 is not shown.

When the obtained populations are inserted into this expression, the magnetization will be $M_z/\gamma\hbar = (76/5)P\delta$ after the fast relaxation. At thermal equilibrium the magnetization is $M_{eq}/\gamma\hbar = 54P\delta$. Thus, when $\omega_t = 2\omega_0$, the level-crossing transitions can create the magnetization equal to (38/135) $M_{eq} = 0.281M_{eq}$ before the other transitions have caused any significant changes in the populations. This value is actually the upper limit because the rate $R_{ta-2} = R$ vanishes when the magnetic field is parallel to the methyl axis. Similar calculations show that at the level crossing $\omega_t = \omega_0$ the transition rates R_{ta-1} and R_{tb-1} can create the magnetization $0.102M_{eq}$.